17th World Conference on Earthquake Engineering, 17WCEE
Sendai, Japan - September 13th to 18th 2020

EXPERIMENTAL INVESTIGATION ON REINFORCED CONCRETE INTERIOR BEAM-COLUMN JOINTS WITH HEADED DIAGONAL BARS

X. Shen[(1)], B. Li[(2)], E.S.S. Lam[(3)]

[(1)] *PhD Student, Department of Civil Engineering, University of Nottingham Ningbo China, xinyu.shen@nottingham.edu.cn*
[(2)] *Assistant Professor, Department of Civil Engineering, University of Nottingham Ningbo China, bo.li@nottingham.edu.cn*
[(3)] *Associate Professor, Department of Civil and Environmental Engineering, The Hong Kong Polytechnic University, siu.shu.eddie.lam@polyu.edu.hk*

Abstract

Beam-column joints (BCJs) have been recognized as the critical elements in reinforced concrete (RC) frame structures as their failure may cause catastrophic collapse of buildings. BCJs are subjected to large shear force during seismic attack and they are normally reinforced with a large number of transverse reinforcements, in accordance with conventional design standards. This brings the problem of reinforcement congestion, construction difficulty, insufficient concrete compaction, and consequently poor seismic performance of BCJs. Although there are attempts to solve the above problems, there is still in lack of practical solution applicable to the construction industry. In this paper, a novel reinforcement method composing headed diagonal bars anchored at beams is proposed. It aims at ameliorating the reinforcement congestion and improving the seismic performance of BCJs. The method involves two mechanisms to enhance the performance of BCJs, namely plastic hinge relocation and shear force reduction. To validate its effectiveness, two 2/3-scale RC interior BCJ specimens were fabricated and tested under quasi-static cyclic loading. The two specimens are identical except the reinforcement at joint region, with one reinforced conventionally and the other adopting the proposed reinforcement method. It is found that the construction of the proposed reinforcement cage is easier than that of its conventional counterpart, as fewer transverse reinforcements were used in the joint core. Test results have shown that the proposed reinforcement method is able to relocate the plastic hinge away from the beam-joint interface and consequently prevents the shear failure of joint core. The BCJ specimen adopting the proposed reinforcement method shows 7.6% increase in loading capacity. Moreover, the proposed reinforcement method enhances energy dissipation and stiffness of BCJs as well as reduces joint deformation. It is generally validated that the proposed reinforcement method can improve both constructability and seismic performance of RC interior BCJs.

Keywords: beam-column joints, headed diagonal bars, plastic hinge, shear force, seismic performance.

1. Introduction

Reinforced concrete (RC) frame structure is one of the most commonly used structural forms for buildings. Among the elements in frame structures, beam-column joints (BCJs) as shown in Fig. 1, play the role of connecting beams and columns as well as transferring loads between them. During an earthquake event, BCJs are subjected to much larger horizontal shear force than their adjacent members. Besides, previous post-earthquake investigations have shown that the deformation of BCJs could contribute up to 60% of story drift [1] and failure of BCJs may even cause global collapse of buildings. Therefore, it is important to have BCJs properly reinforced, and it is now commonly required that failure of BCJs prior to beams and columns shall be avoided.

Fig. 1 – A typical RC interior beam-column joint

BCJs resist shear force in a more complicated way as compared with other structural elements. Since Hanson and Conner [2] revealed that transverse reinforcement is necessary in BCJs, numerous researches were conducted to clarify how BCJs resist shear force. The model proposed by Pauley *et al.* [3] considers that joint shear force is resisted by diagonal concrete strut mechanism and truss mechanism. Strength of concrete strut mechanism is ensured by providing enough section area, and truss mechanism is achieved by proper transverse reinforcements. On the other hand, the ACI 318 [4] regards the BCJs as a part of columns and limits the maximum nominal shear stress as well as specifies a minimum amount of transverse reinforcement for concrete confinement. Although the two approaches calculate the joint shear strength in different ways, both require a certain amount of transverse reinforcement. Moreover, Parate and Kumar [5] reported that modern building codes still overestimate the shear capacity of BCJs. This further indicates that larger amount of transverse reinforcement is required for BCJs. Problems such as reinforcement congestion may occur consequently if the cross section of joint is limited, which further leads to construction difficulty, insufficient compaction of concrete and poor performance of BCJs.

Several attempts have been made to overcome the above-mentioned problems. Choi and Bae [6] estimated the effectiveness of using steel fibers as transverse reinforcement in BCJs, and concluded that using steel fiber in 2% volume fraction to replace code-provisioned transverse reinforcement produces similar seismic performance of BCJs. Lu *et al.* [7] investigated seismic behavior of interior BCJs with various kinds of additional bars, and reported the use of proposed additional bars led to higher strength and ductility of BCJs. However, it is also highlighted that a minimum amount of transverse reinforcement should be provided to ensure the confinement of joint concrete. Saha and Meesaraganda [8] compared the BCJs reinforced using conventional transverse reinforcements or continuous spiral stirrups, and reported that the latter out-performed the former in terms of ultimate strength, stiffness degradation, ductility and energy dissipation.

Another category of method to improve the seismic performance of BCJs is plastic hinge relocation. Additional short steel bars have been proved to be effective in relocating the plastic hinge for exterior and interior BCJs [9,10]. The shifted plastic hinge is beneficial to improving the bonding between beam longitudinal reinforcement and concrete within joint. Lam *et al.* [11] installed unsymmetrical chamfers at the

soffit of beams at beam-column corners, and the loading capacity of BCJs was increased by over 30%. Li *et al.* [12] rehabilitated interior BCJs with ferrocement jackets and obtained 19.8% increase in loading capacity. Arowojolu *et al.* [13] bonded the carbon fiber reinforced polymer to the beam flange of exterior BCJ specimens. Plastic hinge was moved to the curtailment end of the polymer, which enhanced the loading capacity, ductility and stiffness of BCJs.

Although the above-mentioned attempts have been proved to be effective, there is still no practical solution to ease the problem of reinforcement congestion and improving the seismic performance of BCJs. In this paper, a new reinforcement method comprises diagonal bars anchored at beams is proposed. The method involves two mechanisms, namely plastic hinge relocation and shear force reduction. To validate the effectiveness of the proposed reinforcement method, two 2/3-scale interior BCJ specimens were prepared and tested under quasi-static cyclic loading. Seismic performance of the two specimens are evaluated in terms of failure mode, hysteretic behavior, joint deformation and reinforcement strain.

2. Experimental program

2.1 Proposed joint reinforcement method

Conventionally, BCJs are provided with transverse reinforcements evenly spaced along the height of joint region. In this paper, a novel joint reinforcement method is proposed for BCJs as shown in Fig. 2. The method combines the conventional transverse reinforcement with the headed diagonal bars. As shown in Fig. 3, each headed diagonal bar composes of a diagonal part inside the joint and two horizontal anchorage parts. Furthermore, the diagonal part is wrapped with PVC pipe to remove its bonding with concrete, while two steel heads are installed at the ends of horizontal parts to improve their anchorage.

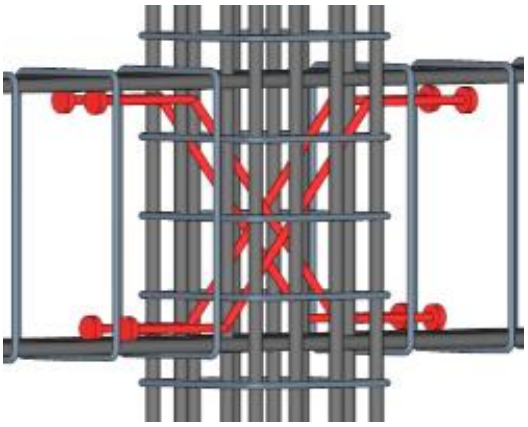

Fig. 2 – Schematic view of the proposed reinforcement method for BCJ

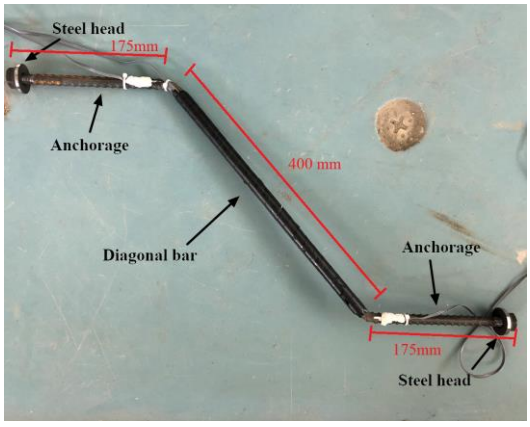

Fig. 3 – Single headed diagonal bar used in the proposed reinforcement

When a BCJ is subjected to a horizontal force, the beam longitudinal bars at diagonal joint edges are under tension or compression. The load taken by beam longitudinal bars will be transmitted into the joint through bonding. Load taken by the horizontal parts of the proposed reinforcement will be transmitted to the diagonal part and is self-balanced as the bonding between diagonal part and concrete is eliminated. Meanwhile, the presence of horizontal parts also increases the flexural capacity of beam section close to the joint, which relocates the plastic hinge to the ends of the proposed reinforcement.

2.2 Specimen description

Two interior BCJ specimens namely BCJ-S and BCJ-D were prepared, whose geometry information and reinforcement details are shown in Fig. 4. The beam has a section of 250 mm ×350 mm with an overall length of 2700 mm. The column has a section of 300 mm ×300 mm with an overall height of 2130 mm. Ready mixed concrete delivered from a local supplier was used. Averaged compressive strength f_{cu} of concrete at 28th day was 24.1 MPa measured using 100 mm cubes. Compressive strength f_{cu} of concrete was also estimated on the loading date of each specimen. Both specimens have identical reinforcements for beams and columns. The beams are symmetrically reinforced with 3Φ14 bars each at top and bottom zones. The columns are reinforced with 8Φ16 bars distributed evenly around its periphery. To prevent shear failure, the beams and columns are deliberately provided with Φ10 transverse reinforcements with a spacing of 100 mm.

The two specimens differ in terms of joint reinforcements. For specimen BCJ-S, three layers of Φ10 transverse reinforcements are provided in the joint core, following the seismic provision specified in GB50010 [14]. The joint reinforcements for specimen BCJ-D comprise one layer of Φ10 transverse reinforcement and four Φ12 diagonal bars. The anchorage length of diagonal bars at beams is 175 mm, corresponding to half of beam height. Hot-rolled ribbed steel bars were used as reinforcements. Measured mechanical properties of steel bars are listed in Table 1.

Table 1 – Measured mechanical properties of steel bars

Diameter (mm)	10	12	14	16
Yield strength f_y (MPa)	450	453	443	460
Ultimate strength f_u (MPa)	635	645	668	650

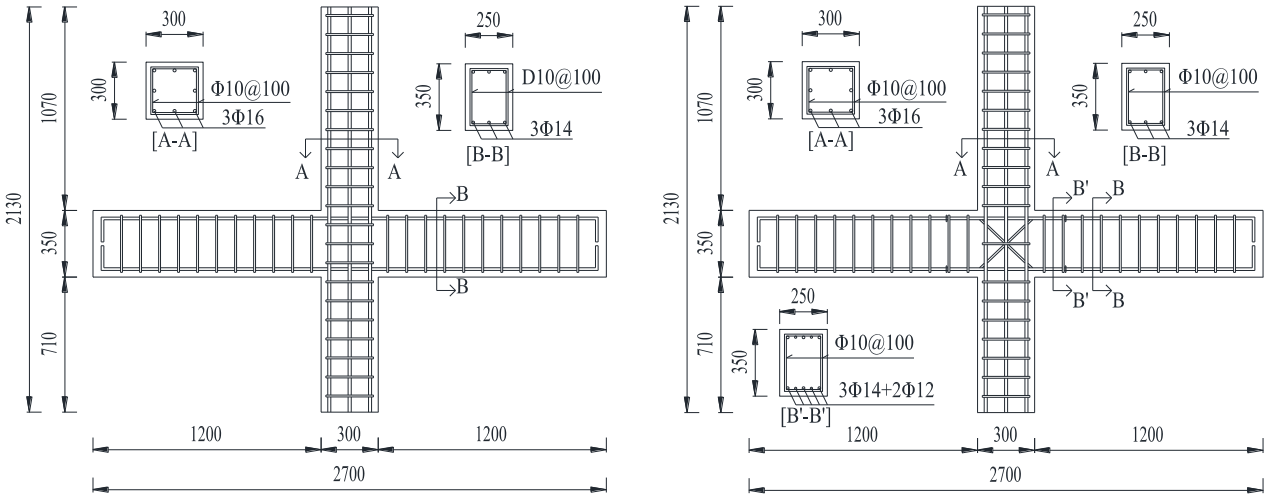

(a) (b)

Fig. 4 – Geometry and reinforcement of specimens (a) BCJ-S and (b) BCJ-D

2.3 Test setup and loading scheme

The two BCJ specimens were tested under quasi-static cyclic load. A schematic view of test setup is shown in Fig. 5. The column was loaded by the method adopted by Yang *et al.* [15]. A hydraulic jack and four post-tension rods were used to apply the axial load on column. The bottom of the column was fixed in a steel fixture hinged to the floor to constrain translational movement only. Both ends of beams were constrained in vertical movement only. A servo-hydraulic actuator was installed at column top to apply the horizonal load. A load cell was installed between the actuator and specimen to monitor the reaction force. At the same height of the actuator, a wire linear variable displacement transducer (LVDT) was placed at the opposite surface of the column to monitor the horizontal displacement. With the above test setup, the distances between contra-flexure points at beam L_b and at column H_c are 2400 mm and 2130 mm, respectively.

The loading sequence for testing specimens consists of two stages. At the first loading stage, a medium level of axial force equal to $0.2f_c'A_g$ was applied, which represents the common loading level for columns [16,17]. Here f_c' is the cylindrical compressive strength of concrete, taken as 0.8 f_{cu} and A_g is the gross section area of the column. At the second loading stage, horizontal displacement was applied by the actuator, following the loading sequence as shown in Fig. 6. At the first cycle, the load was applied to 75% of nominal flexural capacity of beams and the corresponding displacement was recorded as $\Delta_{0.75}$. The assumed yielding displacement Δ_y was then calculated as $\Delta_{0.75}/0.75$. From the second displacement step, the displacement was applied to Δ_y, $2\Delta_y$, $3\Delta_y$, *etc*, with each increment repeated twice. The test stopped until when the horizontal load of specimens dropped to 85% of the loading capacity [18].

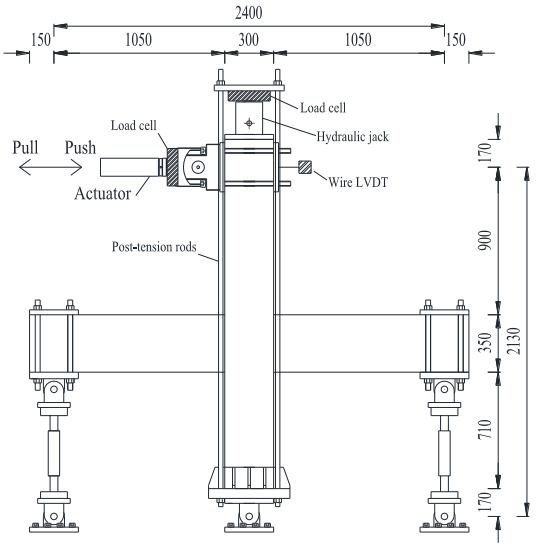

Fig. 5 –Schematic view of test setup for BCJ

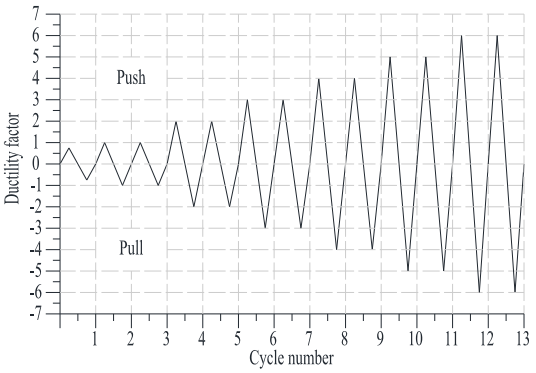

Fig. 6 –Displacement loading history for BCJ

(a) (b)

Fig. 7 – Crack patterns and failure modes of specimens (a) BCJ-S and (b) BCJ-D

3. Results

3.1 General observation and failure mode

Fig. 7(a) shows the crack pattern of specimen BCJ-S after the test. Several hair-line flexural cracks were first found on beams due to the applied bending moment. Two diagonal cracks, one at each direction, were also observed within joint core due to the input shear force at the initial stage of loading. Afterwards, flexural cracks developed and propagated in length and width as the horizontal displacement increased. The measured width of flexural cracks at the beam-joint interfaces reached around 3.0 mm at the displacement of 42.6 mm. Meanwhile, more diagonal cracks appeared in the joint core, but their width were restrained with the shear resistance by transverse reinforcement within joint. Concrete spalling at beam-joint interface first occurred at the displacement of 63.8 mm as the formation of plastic hinge under the reversed loadings. Slight concrete spalling happened at joint core as the horizontal displacement further increased. At the displacement of 106.4 mm, vertical cracks were found at joint edges close to beam-joint interface, caused by the yielding penetration of beam reinforcements. At the end of test, there was a severe concrete spalling within joint region, indicating the shear failure of joint. Overall, specimen BCJ-S failed in beam flexure with formation of plastic hinges followed with joint shear. It indicates that the shear strength of BCJ with conventional trasverse reinforcements was attained before the occurrence of plastic hinges at beam-joint interfaces.

Fig. 7(b) shows the crack pattern of specimen BCJ-D after the test. Similarly, cracks on beams, columns and joint were first observed after the first loading cycle. However, the cracks on the column were more evident than those in specimen BCJ-S, which was caused by the lower flexural capacity ratio of column to beam. The cracks of specimen BCJ-D started to differ from those of BCJ-S when the horizontal displacement reached 42.6 mm. Flexural cracks at the ends of diagonal bars were found to be wider than other cracks on the beams. This was caused by the increased flexural capacity of beam ends due to the incorporation of horizontal parts of diagonal bars. Meanwhile, slight concrete spalling started to appear at beam-joint interface, as the bending moment acting at beam-joint interface was larger. With further increase in displacement, several new shear cracks at joint region were traced but their width almost remained constant. On the other hand, flexural cracks on beams started to concentrate at the sections corresponding to the ends of headed bars, followed by massive concrete crushing. It was obvious that the plastic hinge shifted away from the beam-joint interface to the new critical section at the end of headed bars. Although the joint diagonal cracks within joint core of specimen BCJ-D were quantitatively similar to those of specimen BCJ-S, the joint core in specimen BCJ-D was able to remain its integrity to avoid concrete spalling. In general, specimen BCJ-D failed in beam flexural with plastic hinge developed outside the beam-joint interface.

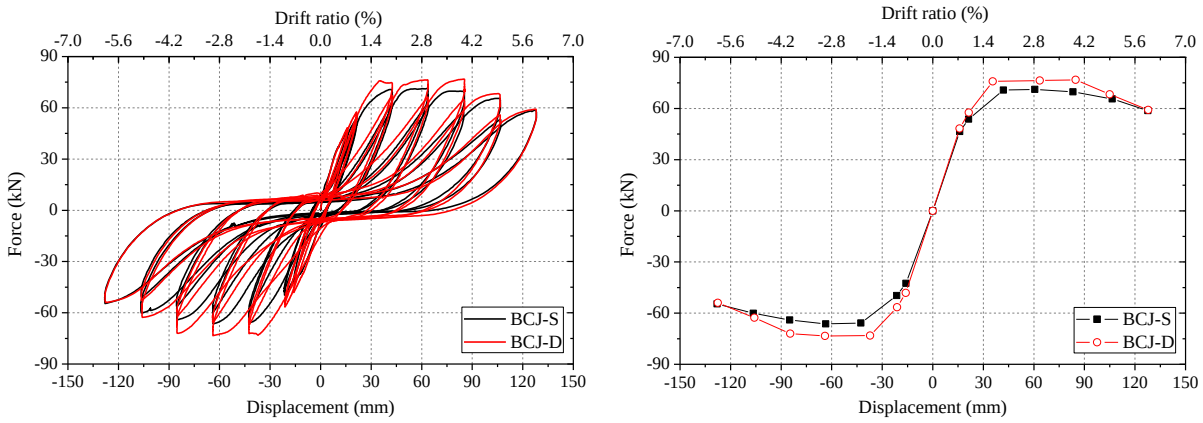

Fig. 8 – (a) Hysteretic loops and (b) envelope curves of specimens BCJ-S and BCJ-D

3.2 Hysteretic behavior and ductility

Fig. 8(a) shows the hysteretic loops for specimens BCJ-S and BCJ-D. In general, both specimens exhibit similar hysteretic behavior, particularly at the first two displacement cycles when the inelastic behavior of specimens is not evident. Afterwards, specimen BCJ-D sustains a higher horizontal load than specimen BCJ-S at the same displacement. This is caused by the relocation of plastic hinge in beams, which reduces the lever arm of forces on the beams. Besides, both specimens suffer severe pinching effect, this might be caused by the degradation of bonding between concrete and beam longitudinal bars due to the relatively low strength of concrete. It highlighted that the strength of concrete could be an essential factor affecting the bonding between concrete and reinforcement, even if the ratio of joint section height over bar diameter satisfies the specification in the code. Nevertheless, the horizontal load of specimen BCJ-D sustained at displacement close to zero is slightly higher than that of specimen BCJ-S. This is probably due to the improved bonding between beam longitudinal bars and joint concrete after the relocation of plastic hinges.

Figure 8(b) shows the envelope curves for specimens BCJ-S and BCJ-D. The envelope curves are obtained by connecting the points corresponding to peak load of the first cycle at each displacement increment. The loading capacity of both specimens are given in Table 2. It can be found that specimen BCJ-D possesses 7.7% and 10.4% higher loading capacity than specimen BCJ-S in push and pull directions. The two curves almost overlap at the initial stage of loading as they remain within the elastic range. Afterwards, the horizontal load sustained by specimen BCJ-D is higher than that of specimen BCJ-S. This is due to the relocation of plastic hinges in specimen BCJ-D that shortens the lever arm for resisting the load. After reaching the peak loads, horizontal load of specimen BCJ-D drops in a faster way as compared with that of specimen BCJ-S. This is mainly caused by the massive concrete spalling at the plastic hinges on beams in specimen BCJ-D.

The displacement ductility can be calculated based on the envelop curves. It is defined as Δ_u/Δ_y, where Δ_u is the ultimate displacement and Δ_y is the yielding displacement. The ultimate displacement Δ_u is defined as the displacement of the point corresponding to 85% of the peak load at descending branch, and the yielding displacement Δ_y is determined by energy balance method [19]. The calculated μ in both push and pull directions for specimens BCJ-S and BCJ-D are shown in Table 2. Compared to specimen BCJ-S, specimen BCJ-D with the proposed reinforcement exhibits slightly smaller ductility. This is attributed to the different failure modes of both specimens. Specimen BCJ-S failed in beam flexural with formation of plastic hinging at beam-joint interface followed by its joint failure at later stage of loading. The failure of specimen BCJ-S distributed along the beam ends and joint region. Specimen BCJ-D failed at the plastic hinges located at ends of headed diagonal reinforcements.

Table 2 – Loading capacity and ductility of specimens

Specimen	f_{cu} (MPa)	P_{peak} (kN)		Δ_y (mm)		Δ_u (mm)		μ		
		Push	Pull	Push	Pull	Push	Pull	Push	Pull	Average
BCJ-S	24.6	71.3	66.4	23.3	23.8	122.0	120.8	5.2	5.0	5.1
BCJ-D	24.4	76.8	73.3	23.0	22.2	112.6	106.8	4.9	4.8	4.9
Note: f_{cu} is the cubic compressive strength of concrete; P_{peak} is the peak horizontal load of specimen.										

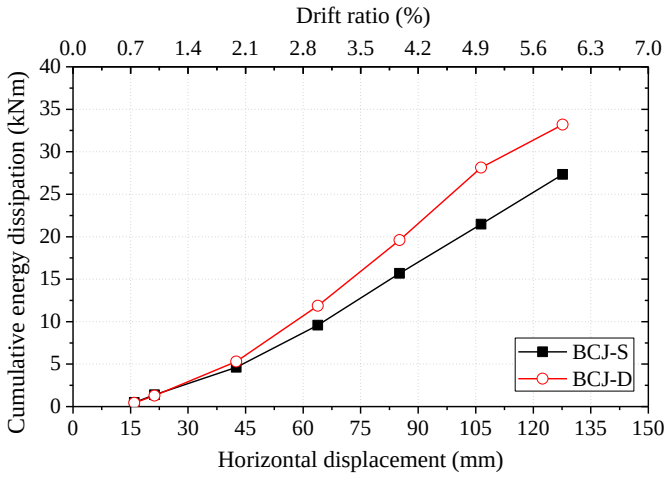

Fig. 9 – Cumulative energy dissipation of specimens BCJ-S and BCJ-D

3.3 Energy dissipation

Fig. 9 shows the cumulative energy dissipation against the horizontal displacement for both specimens. Here, energy dissipation for each loading cycle is estimated by from the enclosed area of each hysteretic loop. The cumulative energy dissipated by both specimens is almost equal before the displacement reaches 21.4 mm. After that, the energy dissipated by specimen BCJ-D becomes higher than that of specimen BCJ-S. This is mainly attributed to the higher load sustained by specimen BCJ-D, due to the relocation of plastic hinges. With further increase in displacement, the proposed joint reinforcement further enhances the energy dissipation of specimen BCJ-D. At the end of the test, the ultimate cumulative energy dissipated by specimen BCJ-D is 21.4% higher than that by specimen BCJ-S.

3.4 Stiffness degradation

Fig. 10 shows the stiffness degradation of the two specimens at the first cycle of each displacement increment. Secant stiffness defined as the slope of the line passing peak points at push and pull directions was calculated and compared. Overall, both BCJ specimens exhibit similar stiffness degradation with the increasing horizontal displacement. However, the stiffness of specimen BCJ-D is slightly higher than that of specimen BCJ-S before failure. This is mainly attributed to the anchorage of diagonal bars which increases the flexural stiffness of beams in specimen BCJ-D. With the occurrence of concrete spalling, the stiffness of specimen BCJ-D deteriorates faster, particularly increasing the displacement from 40 mm to 60 mm. At the end of the test, both BCJ specimens exhibit similar stiffness as they fail in beam flexure or joint shear.

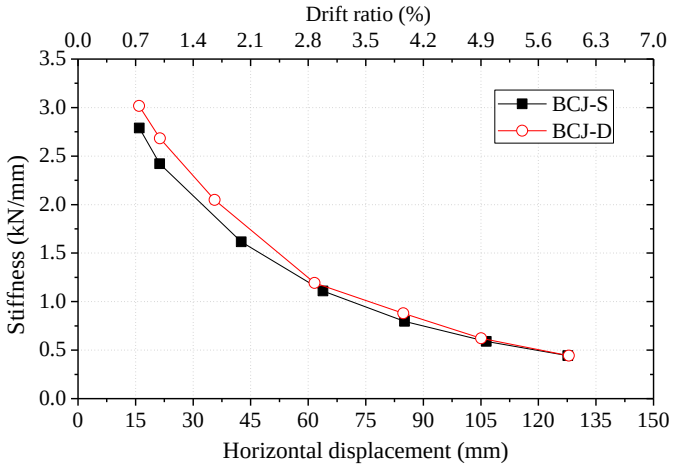

Fig. 10 – Stiffness degradation of specimens BCJ-S and BCJ-D

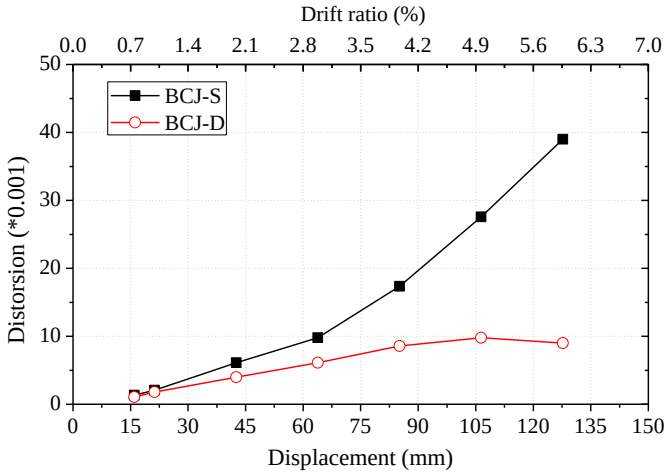

Fig. 11 – Joint distortion of specimens BCJ-S and BCJ-D

3.5 Joint distortion

Fig. 11 shows the joint distortion of specimens BCJ-S and BCJ-D. It is calculated from the deformations in diagonal directions measured by two LVDTs installed at the back of joint region. Both specimens exhibit similar joint distortion before the displacement reaches 21.0 mm. After that, the joint distortion for specimen BCJ-S significantly increases with the horizontal displacement, while that of specimen BCJ-D is properly restrained. This indicates that the relocation of plastic hinge and reduction on joint shear force are able to effectively control the deformation of joint. The joint distortion of specimen BCJ-S increases faster than that of specimen BCJ-D after the displacement reaches 60 mm, which is in agreement with concrete spalling within the joint for specimen BCJ-S. At the later loading stage, the joint distortion of specimen BCJ-D decreases as the horizontal displacement increases. It means that the deformation of specimen BCJ-D is mainly contributed by the plastic hinge rotation rather than joint distortion. It indicates that relocation of plastic hinge away from the joint core in specimen BCJ-D is effective in controlling the joint distortion. At the end of test, the joint deformation of specimen BCJ-S is 4 times than that of specimen BCJ-D.

3.6 Strain on beam longitudinal bars

Fig. 12 shows the strain distribution of upper beam longitudinal bars across the joint region. The strain profiles at displacements of 15.9 mm and 21.3 mm indicate the upper beam longitudinal bars are within the elastic range. It can also be noted that the maximum tensile strain of beam reinforcements for specimen BCJ-

S is located at beam-joint interface, while for specimen BCJ-D is shifted to a distance away from beam-joint interface due to the relocation of plastic hinge. Moreover, tensile strain of beam reinforcements is observed throughout the whole joint region after the displacement reaches 21.3 mm, indicating poor bonding between concrete and beam longitudinal bars within the joint core. This could be caused by the relatively low strength of concrete. Nevertheless, the strain of beam reinforcement in specimen BCJ-D is slightly lower than that of specimen BCJ-S, which reflects lesser shear force in the joint core. Further, the first negative strain occurs at a position closer to the beam-joint interface for specimen BCJ-S, due to the improved bonding after the relocation of plastic hinge.

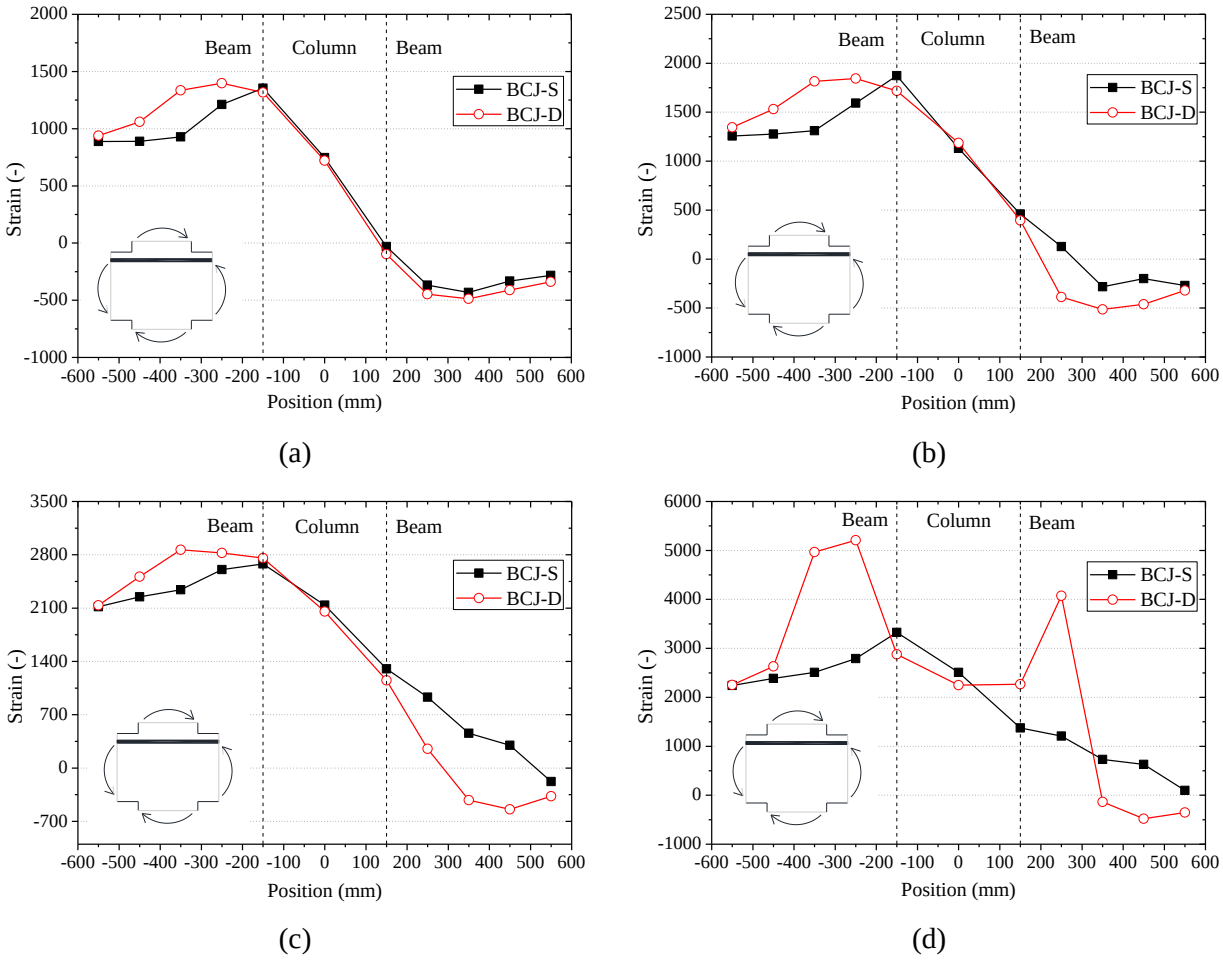

Fig. 12 – Strain profile of upper beam longitudinal bars at the displacements of (a) 15.9 mm, (b) 21.3 mm, (c) 42.6 mm, and (d) 63.9 mm

3.7 Strain on joint transverse reinforcement

Fig. 13 shows the strains of transverse reinforcement within joint core against the horizontal displacement in both BCJ specimens. The strain of transverse reinforcement initially increases with the horizontal displacement as the truss mechanism dominates the joint shear resistance. The strain of transverse reinforcement in specimen BCJ-D is generally smaller than that of specimen BCJ-S, indicating that shear force transmitted from beam longitudinal bars into the joint is reduced. The strain of transverse reinforcement in specimen BCJ-S further increases until the yielding at the displacement of 84.0 mm. However, the strain of transverse reinforcement in specimen BCJ-D starts to decrease after reaching the displacement of 63 mm. This is attributed to that deformation of specimen BCJ-D focuses on the beam plastic hinge. On the other hand, in agreement with the observed joint failure of specimen BCJ-S, the transverse reinforcement within joint core could not sustain the shear force at the later stage. Overall, the

strain of transverse reinforcement within joint core can be reduced for the BCJ with the proposed reinforcement method.

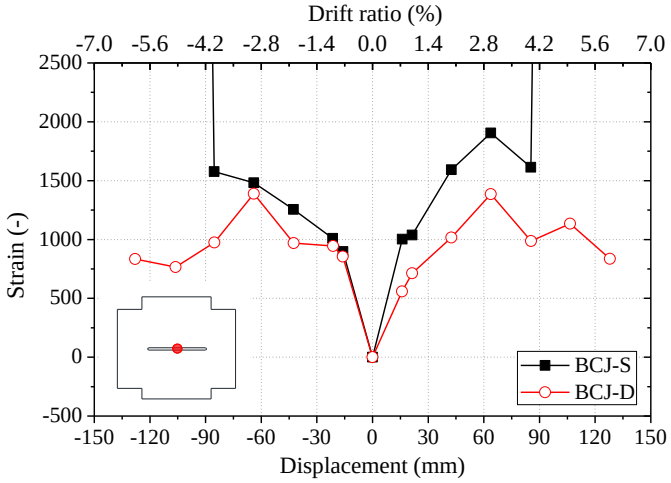

Fig. 13 – Strain on joint transverse reinforcement

4. Conclusion

To solve the problem of reinforcement congestion and improve the seismic performance of BCJs, a novel reinforcement method is proposed for BCJ. Additional diagonal bars were used to replace part of the conventional transverse reinforcement so as to mitigate the joint congestion as well as to improve the behavior of BCJs. Based on the test results, the following conclusions can be made.

(1) The proposed reinforcement method for BCJ is able to relocate the plastic hinge away from beam-joint interface and prevent joint shear failure, which enhances the level of safety for RC buildings.

(2) Compared with conventional reinforcement method, the use of headed diagonal reinforcement increases loading capacity and energy dissipation of BCJ by 7.6% and 21.4%, respectively.

(3) The BCJ with the proposed reinforcements shows higher initial stiffness, but it degrades faster with the development of plastic hinge on beams.

(4) With the headed diagonal reinforcements, the joint deformation can be well controlled and is restrained to 25% of the joint distortion attained by BCJ with conventional reinforcements.

(5) The strain profiles of beam longitudinal bars validate the relocation of plastic hinge on beams and the reduction of shear force transmitted into joint for BCJ with the proposed reinforcements.

(6) The proposed reinforcement method can reduce the strain of transverse reinforcement within joint core due to the reduced joint shear force. This also highlights joint reinforcement can be reduced with the addition of headed diagonal bars.

5. Acknowledgements

This project is supported by the National Natural Science Foundation of China (Grant No. 51708306), Zhejiang Provincial Natural Science Foundation of China (Grant No.: LGF19E080008) and Natural Science Foundation of Ningbo (Grant No. 2018A610354).

6. References

[1] Walker SG (2001): Seismic performance of existing reinforced concrete beam-column joints. (Doctoral dissertation, University of Washington).

[2] Hanson NW, Conner HW (1967): Seismic resistance of reinforced concrete beam-column joints. *Journal of the Structural Division*, **93** (5), 533-560.

[3] Paulay T, Park R, Preistley MJN (1978): Reinforced concrete beam-column joints under seismic actions. *Journal Proceedings*, **75** (11), 585-593.

[4] American Concrete Institute. Committee 318. (1999): *Building code requirements for structural concrete (ACI 318-02) and commentary (ACI 318R-02).* American Concrete Institute.

[5] Parate K, Kumar R (2019): Shear strength criteria for design of RC beam–column joints in building codes. *Bulletin of Earthquake Engineering*, **17** (3), 1407-1493.

[6] Choi CS, Bae BI (2019): Effectiveness of Steel Fibers as Hoops in Exterior Beam-to-Column Joints under Cyclic Loading. *ACI Structural Journal*.

[7] Lu X, Urukap TH, Li S, Lin F (2012): Seismic behavior of interior RC beam-column joints with additional bars under cyclic loading. *Earthquake and Structures*, **3** (1), 37-57.

[8] Saha P, Meesaraganda LV (2019): Experimental investigation of reinforced SCC beam-column joint with rectangular spiral reinforcement under cyclic loading. *Construction and Building Materials*, 201, 171-185.

[9] Park R, Milburn JR (1983): Comparison of recent New Zealand and United States seismic design provisions for reinforced concrete beam-column joints and test results from four units designed according to the New Zealand code. *Bulletin of the New Zealand national society for earthquake engineering*, **16** (1), 3-24.

[10] Hwang HJ, Eom TS, Park HG (2015): Design considerations for interior RC beam–column joint with additional bars. *Engineering Structures*, 98, 1-13.

[11] Lam ESS, Li B, Xue ZH, Leung KT, Lam JYK (2019): Experimental studies on reinforced concrete interior beam-column joints strengthened by unsymmetrical chamfers. *Engineering Structures*, 191, 575-582.

[12] Li B, Lam ESS, Wu B, Wang YY (2013): Experimental investigation on reinforced concrete interior beam–column joints rehabilitated by ferrocement jackets. *Engineering Structures*, 56, 897-909.

[13] Arowojolu O, Ibrahim A, Rahman MK, Al-Osta M, Al-Gadhib AH (2019): Plastic hinge relocation in reinforced concrete beam–column joint using carbon fiber–reinforced polymer. *Advances in Structural Engineering*, **22** (14), 2951-2965.

[14] China Academy of Building Research (2015): *Code for design of concrete structures. GB50010.* China Building Industry Press, 2015 edition.

[15] Yang H, Zhao W, Zhu Z, Fu J (2018): Seismic behavior comparison of reinforced concrete interior beam-column joints based on different loading methods. *Engineering Structures*, 166, 31-45.

[16] Alaee P, Li B, Cheung PP (2015): Parametric investigation of 3D RC beam–column joint mechanics. *Magazine of Concrete Research*, **67** (19), 1054-1069.

[17] Al-Osta MA, Khan U, Baluch MH, Rahman MK (2018): Effects of Variation of Axial Load on Seismic Performance of Shear Deficient RC Exterior BCJs. *International Journal of Concrete Structures and Materials*, **12** (5), 683-702.

[18] China Academy of Building Research (2015): *Specification for seismic test of buildings. JGJ/T 101-2015*. China Building Industry Press, 2015 edition.

[19] Lam SSE, Wu B, Wong YL, Wang ZY, Liu ZQ, Li CS (2003): Drift capacity of rectangular reinforced concrete columns with low lateral confinement and high-axial load. *Journal of Structural Engineering*, **129** (6), 733-742.

